http://pubs.acs.org/journal/acsodf Article

Modeling of Coke Distribution in a Dry Quenching Zone

Serhiy Pyshyev,* Yevgen Zbykovskyy, Iryna Shvets, Denis Miroshnichenko, Sergiy Kravchenko, Stanislav Stelmachenko, Yuriy Demchuk, and Nataliya Vytrykush

Cite This: *ACS Omega* 2023, 8, 19464–19473

Read Online

ACCESS | Metrics & More | Article Recommendations

ABSTRACT: Herein, a method for the coke dry quenching (CDQ) process has been proposed and its optimization has been carried out, which will minimize the disadvantages of this process. This optimization was carried out to develop a technology for uniform coke distribution in the quenching chamber. A model of the real charging device for quenching coke from the Ukrainian enterprise PrJSC "Avdiivka Coke" was developed, and several shortcomings of its operation were shown. It is proposed to use a coke distributor in the form of a bell and a modified bell (specially shaped holes). Graphic mathematical models of the operation of these two devices were developed, and the efficiency of the last of the developed distributors was shown.

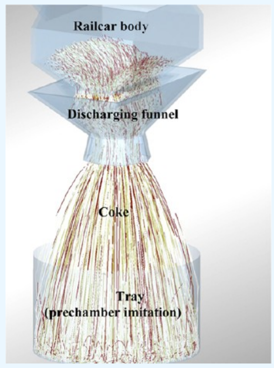

1. INTRODUCTION

The coke industry is one of the essential industries and provides coke to ferrous metallurgy and several other sectors. Using coking, the chemical processing of hard coal of different grades and levels of oxidation is carried out.[1,2] Together with coke, high-calorie coke gas and liquid products containing various valuable substances, primarily aromatic ones, are obtained.[3−7] The main areas of coke application include iron smelting, the foundry industry, recovery of non-ferrous ores, and sintering of charge materials.[3−5]

The blast furnace coke must have lump sizes of at least 40 mm with a limited lump content of less than 25 mm (no more than 3%) and no more than 80 mm. These lump sizes are due to the fact that the blast furnace is a shaft-type furnace in which gases and charge materials are countercurrent. If the coke pieces are smaller than the required size, they will be removed from the furnace along with the gases.

The coke coming out of the furnace is quenched (cooled to 180−250 °C) because it is in a red-hot state (with a temperature of 950−1000 °C). The method and technique of quenching significantly affect its subsequent strength and therefore the size of the pieces.[8,9]

There are two quenching methods: wet and dry.[10] In the wet method, coke is sprayed with a certain amount of water in the quenching tower. The formed water vapor is removed through the exhaust pipe.

During dry quenching, coke is cooled by CO_2 or N_2. In this case, the coke through a special charging facility is fed into the coke dry quenching (CDQ) installation, which consists of a quenching chamber divided into two parts, a cyclone in which dust is separated, a boiler-utilizer and a blower. An almost constant temperature is maintained in the upper part of the quenching chamber (prechamber). The prechamber usually contains coke from three to five ovens for 40−60 min. Prechambers serve to equalize the temperature throughout the coke mass. This is necessary for supplying coke with the same temperature to the cooling zone, which, in turn, will allow the inert heat-carrying gas with a constant temperature to be removed. After the coke passes through the gas pipeline zone, it reaches the inert gas and cools to a temperature of 250−280 °C. Coke is unloaded through a special discharging device in portions of 20−30 kg. The inert gas at a temperature of 760−800 °C enters the cyclone for dust separation, passes through the boiler-utilizer, and, cooled to 180−200 °C by the smoke extractor returns to the quenching chamber distribution device—the distributor.

The advantages of wet quenching are low capital costs and no dusting of coke during sorting and discharging. Disadvantages include complete heat losses from hot coke (40% of the total heat consumption for coking) and pollutant emissions into the atmosphere from the quenching tower. In addition, the rapid cooling of coke with water leads to its intensive cracking, a decrease in the yield of coarse coke and its quality deterioration, and intensive corrosion of metal structures in the

Received: February 5, 2023
Accepted: May 5, 2023
Published: May 19, 2023

https://doi.org/10.1021/acsomega.3c00747
ACS Omega 2023, 8, 19464–19473

area of the quenching tower. Also, disadvantages include substance emissions that have an extremely harmful effect on the environment together with water vapor from the quenching tower, namely, phenol, ammonia, hydrogen cyanide, sulfur, and carbon oxides.

Dry quenching has a number of important advantages: absence of pollutant emissions into the atmosphere from the quenching tower; the possibility of providing coke chemical production with steam and electricity due to the utilization of the heat of red-hot coke; minimum coke moisture; obtaining a more homogeneous coke in terms of size; improving the quality of coke due to the absence of rapid cooling; corrosion prevention of metal structures in the area of the quenching tower. Dry quenching compared to wet quenching allows the reduction of coke moisture content by 3−4%, improves mechanical strength indicators—for M_{25} by 4−6% and for M_{10} by 0.3%—, and reduces the content—of the grade greater than 80 mm in coke by 3−4% and for the class less than 25 mm by 0.1%. In blast furnace production, the specific consumption of CDQ is 2−3% lower than that of coke wet quenching. Moreover, the use of dry quenching improves such indicators of blast-furnace coke as the coke reactivity index (CRI) and CSR (coke strength after reaction with CO_2), the values of which largely determine the consumption of blast-furnace coke in a blast furnace.[11]

At the same time, certain risks are inherent in CDQ, namely, large capital costs; loss of part of the coke due to gasification in the chambers; increased coke dust; additional pollutant emissions into the atmosphere with excess circulating gas.

Optimization of the CDQ process will allow minimizing the abovementioned disadvantages. Works on improving the CDQ process are carried out in various directions.[12−18] One of the directions for such optimization is the technology development for the uniform distribution of coke in the quenching chamber. Therefore, the research purpose described in the article is to find a solution in which each class of coke will be evenly distributed across the section of the quenching chamber.

2. EXPERIMENTAL SECTION

The research consisted of studying the distribution of coke porosity in the quenching zone and the degree of influence on its various devices involved in loading and was carried out by the method of discrete elements.

Based on the statement that the pressure loss when passing through a layer of coke strongly depends on the size of its particles, it was suggested that the efficiency of coke cooling depends on the gas permeability of the charged coke, which is affected by the porosity (the fraction of free space between the particles). That is, it was necessary to determine what the porosity depends on and how it is distributed in the charged coke.

Practical data obtained at PrJSC "Avdiivka Coke" indicate the porosity dependence on the concentration of the different-size particles. At the same time, changes in porosity are enhanced due to particle size segregation as a result of shrinkage. The greatest compaction is observed in the center of filling coke, and the largest amount of coke material is found (coke, falling from a great height to one-point, self-compacts in this area). That is, the porosity in the quenching zone is affected not only by the size distribution of coke but also by compaction from a great height falling. That is, by correctly choosing the form of devices and methods of charging/discharging coke, it is possible to achieve the maximum uniform distribution of small and large classes of coke during its dry quenching.

To obtain reliable data, it was important to simulate as accurately as possible the conditions of real coke charging first into the railcar, then into the chamber, as well as the conditions in the chamber itself. Therefore, the following algorithm was developed:

- simulation of charging coke from the coking chamber into the railcar;
- discharging coke from the railcar through a facility whose dimensions correspond to the upper part of the storage chamber;
- studying the flow properties and transferring the projection of its intersection to the surface that generates coke falling into the chamber quenching zone;
- charging coke into the camera. The charging process was divided into stages to reduce the simulation space size and finite element mesh. Study of the distribution of coke porosity in the chamber;
- transferring the results to ANSYS FLUENT, which is a package of programs created by ANSYS, Inc. company. The package allows us to solve a wide range of problems in the areas of strength, heat, hydro-gas dynamics, and electromagnetism, as well as interdisciplinary analysis that combines all four areas.

The installation model, which was used as a base for the development of coke distribution parameters, is presented in Figure 1.

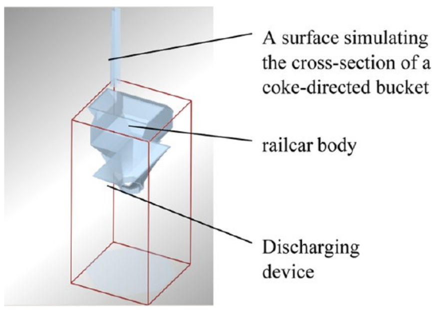

Figure 1. Installation model.

The model includes an imitation of the coke-directed bucket, which is located above the coke-carrying railcar at the time of coke discharge. At the same time, the railcar body is pre-positioned directly above the quenching chamber. The bottom of the railcar is initially closed. The surface, which is the cross-section of the coke-directed bucket, generates coke particles uniformly distributed in size over the entire height and width (Figure 2).

After loading the coke into the rail and waiting for 10 s (for the coke shrinkage in the railcar), the bottom is opened and the coke is discharged into the quenching chamber. At the level of the lower coke sensor, there is a tray with a diameter of 5270 mm for catching particles. Loading the railcar lasted 40 s.

The shape of the average coke particle, which was used in the calculations, is shown in Figure 3, and the ratio of its sides is in Table 1.[19] Table 2 shows the geometric dimensions of the ramp coke PrJSC "Avdiivka Coke" particles, and Table 3 shows the coke used for simulation. Since the small classes' behavior is similar to that of dust, which distorts the result, in this coke, the small classes are excluded and transformed into larger ones.

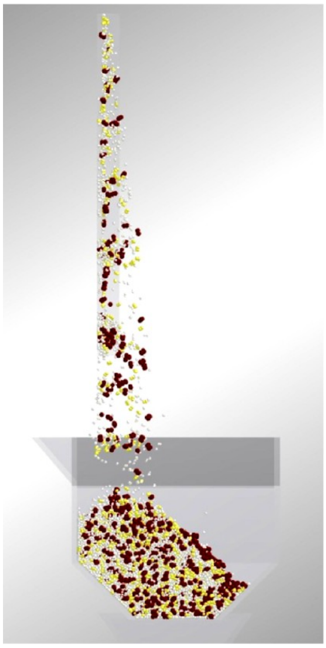

Figure 2. Coke-directed bucket imitation model, which is located above the coke-carrying railcar during coke discharge.

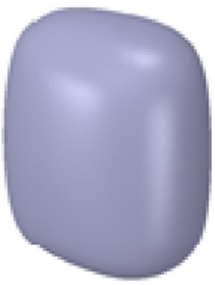

Figure 3. Shape of an average coke particle (parallelepiped).

Table 1. Side Ratios of the Coke Particle

length	width	height
1.346	1.000	0.757

Table 2. Sizes of Ramp Coke Particles

class, mm	>80	80–60	60–40	40–25	25–10	<10
yield, %	48.7	25.0	15.7	5.3	2.1	3.2

Table 4 shows the coefficients of restitution (COR), static friction (CSF), and rolling friction (CRF) used in the simulation, and Figure 4 shows the location of coke in a coke-carrying railcar.

The coefficient of static friction in coke corresponds to an angle of 37°.

Table 4. COR, Static Friction, and Rolling Friction

coefficient	coke/coke	coke/steel	coke/refractory
COR—restitution	0.40	0.30	0.20
CSF—static friction	0.75	0.17	0.26
CRF—rolling friction	0.26	0.10	0.18

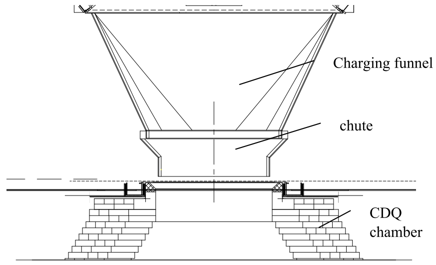

Figure 4. Real coke charging device of PrJSC "Avdiivka Coke".

The smallest porosity of the stationary layer for the composition given in Table 2, calculated by the Syskov formula,[19] is equal to 0.627 m^3/m^3

$$\varepsilon_c = 0.0005\cdot\sum_{i=1}^{n} a_i\cdot x_i = 0.0005\cdot(15.5\cdot48.7 + 11.3\cdot25 + 9.1\cdot15.7 + 7.6\cdot5.3 + 6.7\cdot2.1 + 6.3\cdot3.2) = 0.627\ \mathrm{m^3/m^3} \quad (1)$$

For the composition used for simulation (Table 3), it was set to 0.633 m^3/m^3

$$\varepsilon_c = 0.0005\cdot\sum_{i=1}^{n} a_i\cdot x_i = 0.0005\cdot(15.5\cdot48.7 + 11.3\cdot25 + 9.1\cdot19.7 + 7.6\cdot6.6) = 0.633\mathrm{m^3/m^3} \quad (2)$$

In the above formulas: a_i—empirical coefficient; x_i—yield of i-class.

Both values are almost identical. Thus, the use of the coke sieve composition accepted in the model is correct for this simulation.

3. RESULTS AND DISCUSSION

3.1. Development of a Model of the Real Charging Device Used in PrJSC "Avdiivka Coke". Figure 4 shows the real charging device used in PrJSC "Avdiivka Coke".

Figures 5–8 show the stages of charging coke into the chamber.

The particle velocity varies from 12 to 11.5 m/s at the level of the lower sensor. Figure 9 shows histograms of the coke particle size distribution. Red color corresponds to the highest concentration and blue to the lowest. Coke is collected in a tray with a diameter equal to the accumulation chamber diameter—5270 mm.

Table 3. Coke Particle Sizes Transformed for Simulation

	sizes of coke particles, mm				volume, m^3	mass, kg	
class, mm	length	width	height	diameter	V	M	yield, %
>80	134.60	100.00	75.70	124.87	0.001019	0.8864	48.7
60–80	94.22	70.00	52.99	87.41	0.000349	0.3041	25.0
40–60	67.30	50.00	37.85	62.43	0.000127	0.1108	19.7
<40	26.92	20.00	15.14	49.38	0.000063	0.0548	6.6

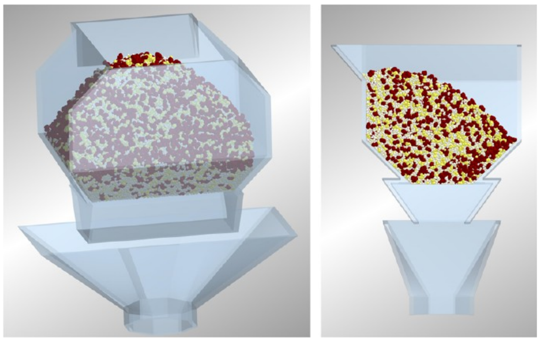

Figure 5. Coke before charging into the CDQ chamber.

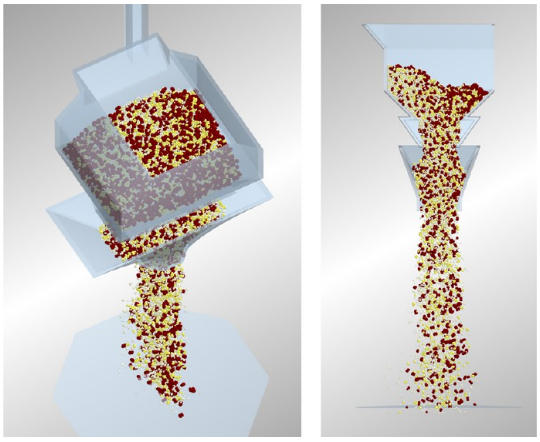

Figure 6. Start of coke charging into the CDQ chamber.

Figure 9 shows that small coke particles are concentrated on the side from which the filling was carried out at the stage of loading coke into the railcar. Large particles, being segregated, move to the opposite side. This effect may be slightly greater in production due to the presence of smaller classes.

The process of segregation of blast-furnace coke particles during their fall can be caused by several factors. This can lead to the formation of different areas, sizes, and densities.

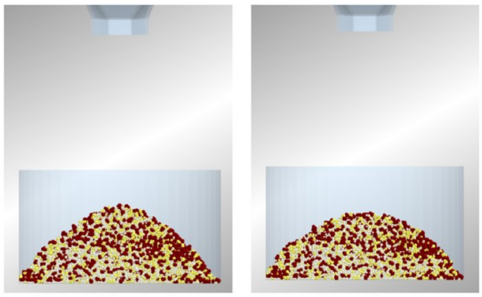

Figure 8. "Surface" of coke.

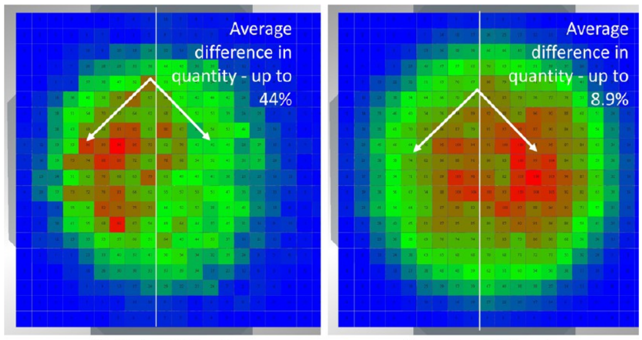

Figure 9. Distribution of coke pieces immediately after filling in the tray on the embankment lower part.

Due to quite predictable behavior of coke particles in the numeral experiment conditions, variation analysis did not required.

It can be seen in Figure 10 that the porosity inside the outer ring has an unevenness of up to 3.5%, and the deviations between the center and the outer ring reach 8.0%.

According to Figure 10, it can be concluded that the porosity depends on the concentration of different size particles. At the same time, porosity changes are enhanced due to particle size segregation as a result of shrinkage.

Nevertheless, the greatest shrinkage was in the center of the backfill, where the largest amount of coke material was found,

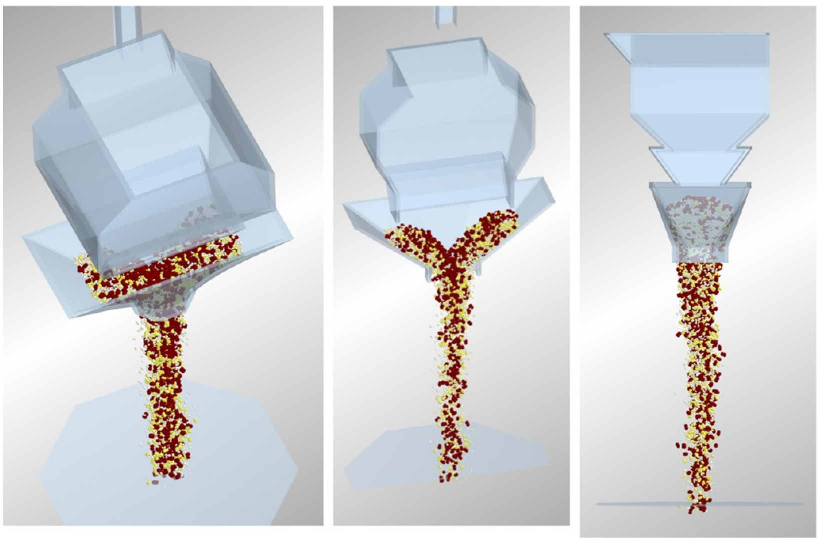

Figure 7. End of coke charging.

https://doi.org/10.1021/acsomega.3c00747
ACS Omega 2023, 8, 19464−19473

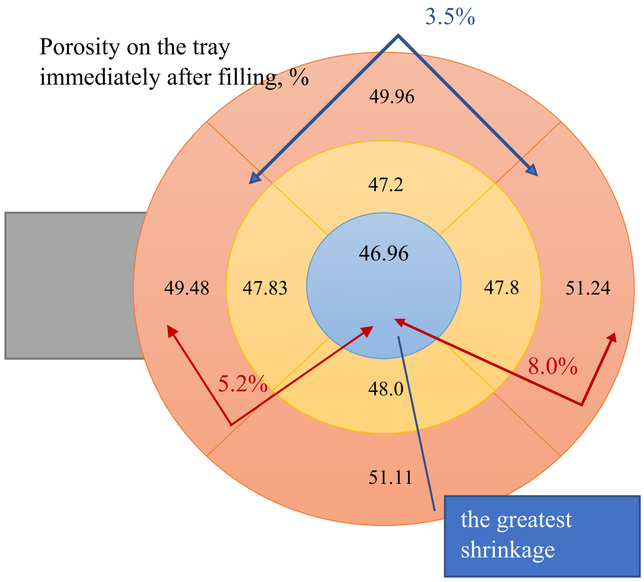

Figure 10. Distribution of porosity per tray and percentage difference.

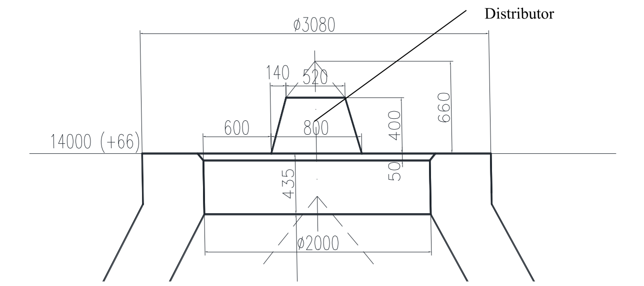

Figure 11. First design of the coke distributor in the funnel of the loading hole.

that is, falling from a great height to one point, the coke self-compacts in this zone. Thus, porosity in the quenching zone is affected not only by the size distribution of coke but also by compaction from a great height falling. And this has a stronger effect on porosity than segregation.

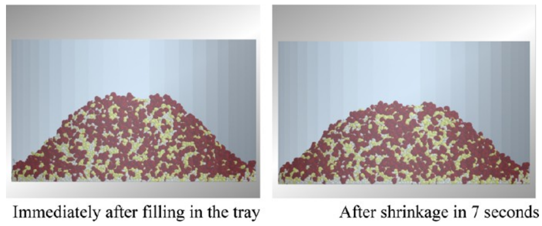

Figure 13. Coke embankment.

3.2. Modeling of a Bell-Shaped Coke Distributor. The first proposed alternative bell-shaped coke distributor had a diameter of 800 mm and a surface angle of 75° (Figure 11). Figure 12 shows the stages of coke descent through the developed distributor.

The selected 800 mm diameter and shape distributor did not create a sufficient size funnel within the backfill (Figure 13) to eliminate residual segregation. It also had little effect on the distribution uniformity of small and large classes to the coking chamber location.

The size distribution of coke particles at the level of the lower sensor until the end of the experiment when they enter the tray is shown in Figures 14 and 15.

It can be seen in Figures 14 and 15 that the class of large particles in the case of using the new charging device is distributed more evenly around the chamber perimeter in comparison with the usual charging device, which is a positive effect as it reduces the coke segregation by size.

To further enhance this effect, it made sense to test a distributor with an increased diameter and a different inclination angle of the working surface.

3.3. Modeling of a Charging Device with a Modified Coke Distributor. As a result of a series of experiments, the second alternative form of the distributor and outlet of the funnel gap was selected (Figure 16).

The main criteria for choosing the design of the distributor and funnel gap are:

- coke descent time from the funnel (should not increase);

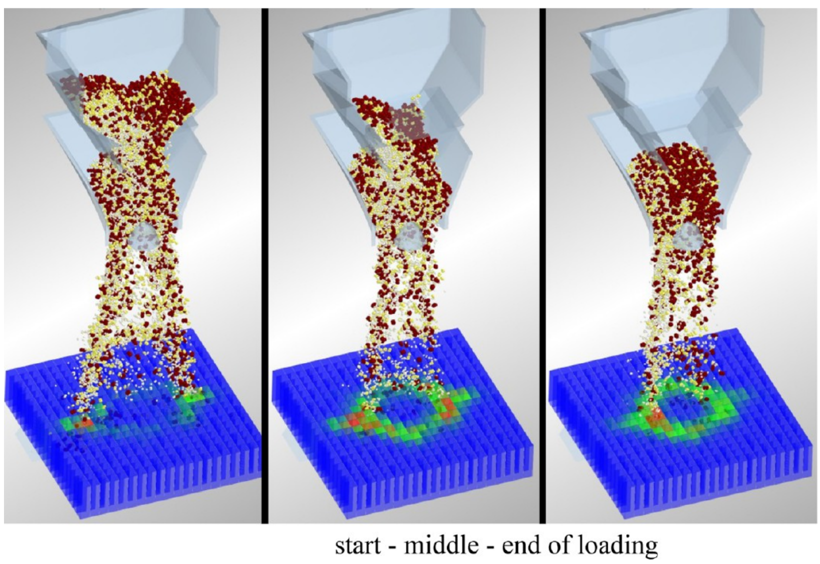

Figure 12. Stages of coke descent through the proposed distributor.

https://doi.org/10.1021/acsomega.3c00747
ACS Omega 2023, 8, 19464−19473

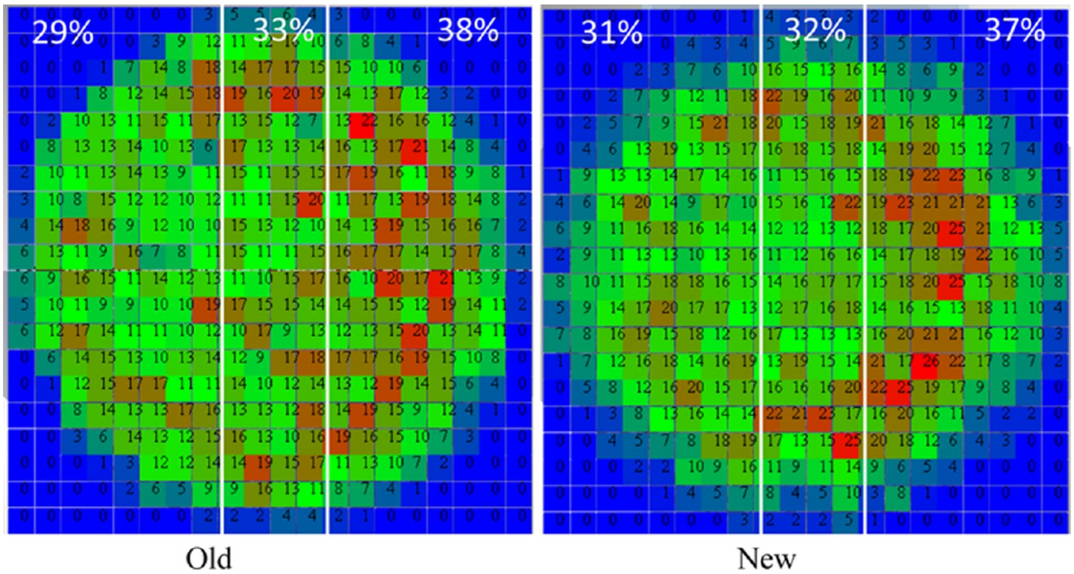

Figure 14. Comparison of particle distribution at the end of the experiment with old and new charging devices. Class of large (+60 mm) particles.

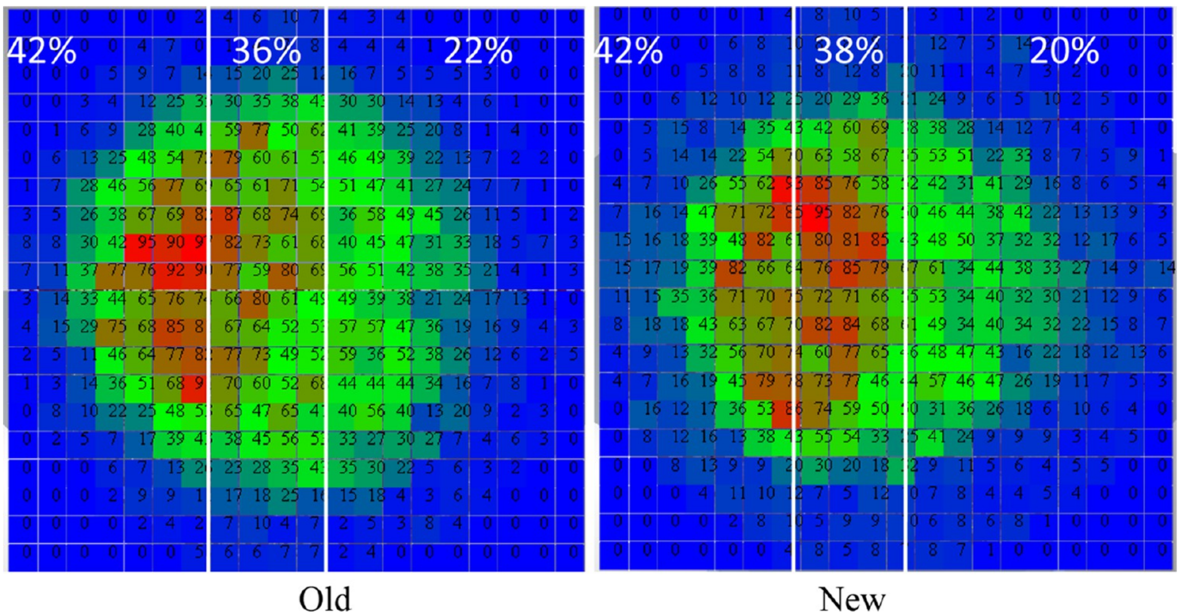

Figure 15. Comparison of particle distribution at the end of the experiment with old and new charging devices. Class of small (−60 mm) particles.

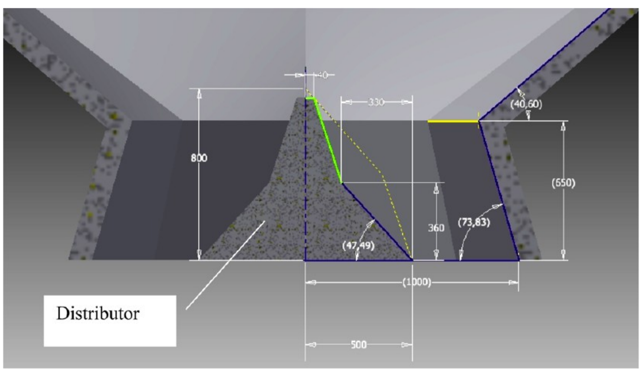

Figure 16. Changed coke distributor and funnel hole.

- particle distribution diameter (must be large enough that large particles can roll to the funnel center).

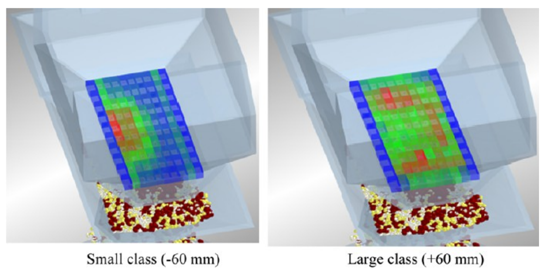

Figure 17. Coke size distribution during discharge from the railcar (number of particles indicated by color: red—79÷95, brown—68÷78, light green—43÷67, dark green—27÷42, dark blue—5÷10).

The emptying time of the old design discharging funnel of PrJSC “Avdiivka Coke” was 12.8 s (average consumption 744.6 kg/s). The emptying time of the new design funnel was 13.5 s (average consumption 592.6 kg/s).

https://doi.org/10.1021/acsomega.3c00747
ACS Omega 2023, 8, 19464−19473

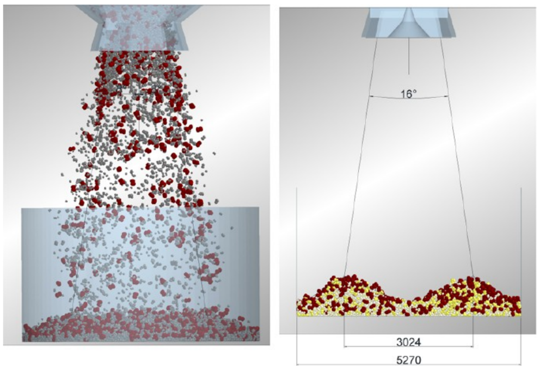

Figure 18. Particle dispersion angle.

This time cannot be directly compared to the actual time because it was not possible to simulate the full railcar loading.

The following was established during the experiments:

1 the funnel diameter in the upper part of the passage hole is decisive for the discharging time and should not be less than 1500 mm because in this part the particle flow is compacted (the diameter adopted by us is 1620 mm);
2 reducing the funnel inclination angle from 43 to 40° practically does not affect the descent velocity;
3 the distributor diameter can be increased more because the flow of particles is rarefied in the lower part of the funnel;
4 the inclination angles of the distributor's lower part and the funnel's lower part determine the particle dispersion angle;
5 the beam for fixing the distributor should be as narrow and sharp as possible to prevent the possible residual hanging of coke particles on it after the passage of the entire mass.

In the simulation, the same railcar with the same loaded amount of coke particles as in the previous experiments was used. A more detailed analysis showed a noticeable unevenness in the distribution of particles in the output hole of the railcar after the coke was got out of it (Figure 17).

The particle dispersion angle was 16° (Figure 18). Above the level of the lower sensor, the top of the formed funnel is a circle with a diameter of 3.0 m.

It should be noted that at the initial moment, the dispersion angle was quite large and amounted to 40°. But after 0.5 s, it was 30°, and after another 0.75 s, it was 16°, and it did not change until the end of the funnel emptying (Figure 19). The reason for the large initial dispersion angle is the large kinetic energy of the first pieces of coke, which do not encounter barriers on their trajectory. As the number of pieces increases, they begin to interact with each other, especially at the exit from the funnel, due to which the momentum vectors change, kinetic energy is spent on collisions, and the average velocity in the direction of movement decreases.

To prevent this from happening, it is necessary to carry out a pick-off on the outer wall in the lower part of the funnel outlet hole, which equalizes the coke flow. The average speed of falling particles directly before the distributor is about 2 m/s, and at the level of the lower sensor it is 11.7 m/s (Figure 20).

For further conclusions, the particle flow directly above the tray was simulated as a continuation (second stage) of backfilling.

To do this, an analysis of the particle distribution in the coke flow on the approach to the tray was carried out. The flow was conventionally divided into sectors, and the number of particles in each sector was calculated and included in the total number of particles of the same name (Table 5). The ratios were converted to mass consumption.

The average velocity of particles at this level was 8.754 m/s.

A surface consisting of sectors containing particles in the required ratio was created above the tray (Figure 21).

The movement of a single marked coke particle (orange color) is shown in Figure 22.

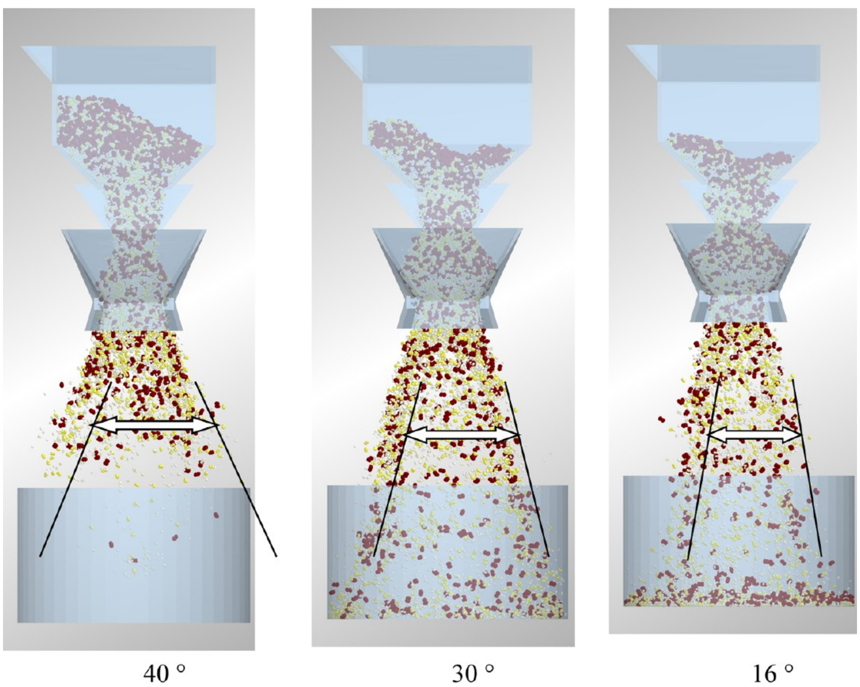

Figure 19. Change in particle dispersion angle during coke discharging.

https://doi.org/10.1021/acsomega.3c00747
ACS Omega 2023, 8, 19464−19473

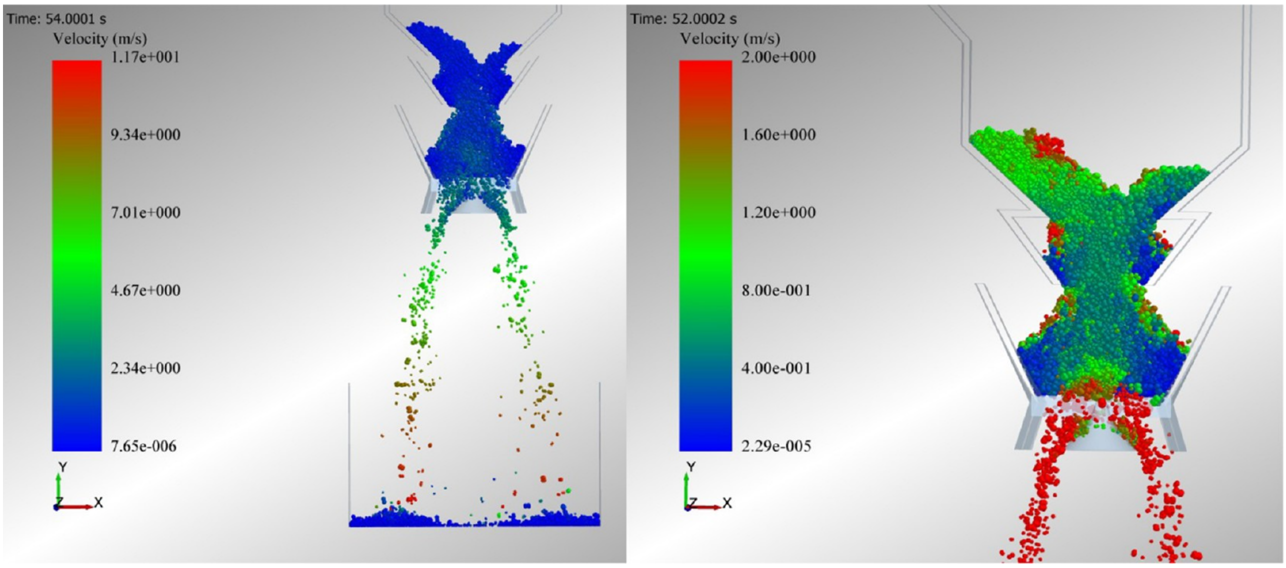

Figure 20. Fall velocity of particles.

Table 5. Initial Particle Size Distribution in the Coke Flow before the Tray

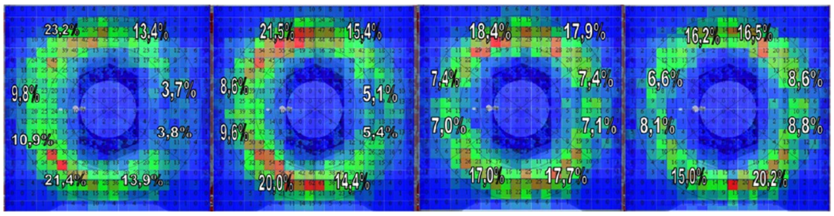

class	<40	60–40	80–60	>80
D particles, mm	49.4	62.4	87.4	124.9

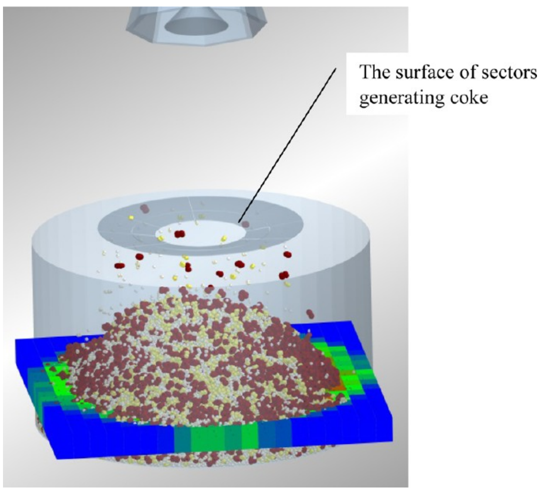

Figure 21. Creation of the backfill surface.

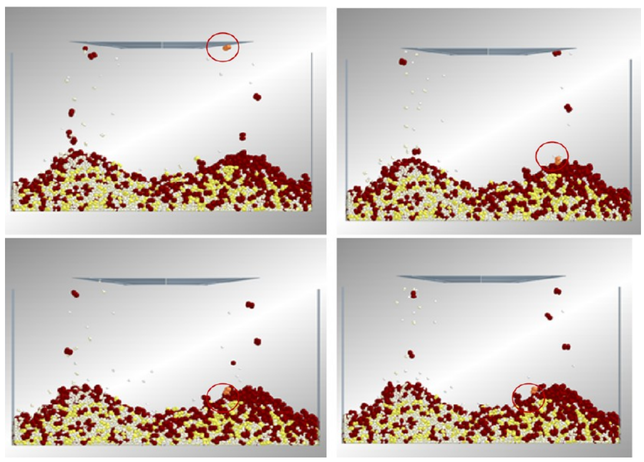

Figure 22. Movement of individual coke particles.

After falling, the movement of the particle toward the central axis of the camera is observed.

This is also confirmed by the statistical analysis of particle distribution on the funnel (Figures 23 and 24).

Particles of all classes are redistributed along the funnel circle.

Both small and large classes after falling move to the central axis of the camera and the periphery. But to the central axis is a greater extent, perhaps due to the asymmetry of the inner and outer slopes of the formed funnel. Large particles move to the center more actively because they have a greater momentum

$$\vec{P} = m\vec{V} \quad (3)$$

m—particle's mass (larger for coarser particles), $\vec{V}$—its velocity.

At the same time, a gap is formed along the central axis through the asymmetry of the outer and inner slopes of the backfill.

https://doi.org/10.1021/acsomega.3c00747
ACS Omega 2023, 8, 19464−19473

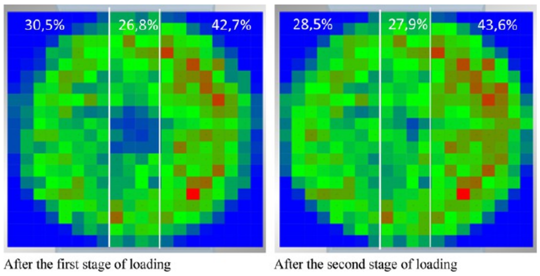

Figure 23. Distribution of large (+60) class particles (number of particles indicated by color: red—27÷30, brown—21÷26, light green—17÷20, dark green—11÷16, dark blue—3÷10).

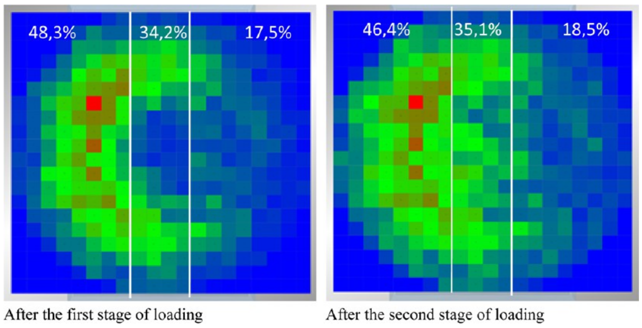

Figure 24. Distribution of small (−60) class particles (number of particles indicated by color: red—79÷95, brown—68÷78, light green—43÷67, dark green—27÷42, dark blue—5÷10).

The gap in the coke turned out to be saddle-shaped, symmetrical relative to the plane of the beam on which the distributor was attached (Figure 25). It was assumed that the beam itself influenced the shape of the gap. However, it later turned out that with such a design, when the beam is raised above the distributor sole, its influence is minimal. The reason is mainly due to the different slopes of the charging funnel. Steeper slopes accumulate coke, and it comes off them more slowly, gradually adding to the general flow.

Thus, the selected shape and dimensions of the distributor and the loading funnel, shown in Figure 16, ensure the scattering of particles with their subsequent stacking in the form of a gap inside the chamber. The gap ensures the dispersion of particles and their gradual movement toward the central axis during the loading.

4. CONCLUSIONS

The following aspects affecting the efficiency of coke quenching were established, namely: the probability of coke under-quenching when it passes through the distributor; the dynamic compaction of coke due to the fall of a large mass on the same area from a great height; the segregation effect (difference in the rate of coke rising opposite the distributor due to different concentrations of small and large particles with different momentum in different parts of the chamber) as a result of the uneven distribution of equivalent diameters of coke particles in different areas of the chamber.

It was established by the proposed damping unevenness coefficient that the most negative phenomenon is an ascent rate increase in the chamber opposite the blowing device on the side where the concentration of small particles is higher. Therefore, new solutions should be aimed primarily at eliminating particle size segregation.

The use of a coke distributor in the form of a bell in the loading funnel allows dispersing of small classes in the form of a ring near the walls, which contributes to the acceleration of the rise of coke in these areas and the slowdown in the center.

The selected shape and dimensions of the distributor in the form of a modified bell (special-shaped gaps) ensure the scattering of particles with their subsequent stacking in the form of a gap inside the chamber. The gap ensures the dispersion of particles and their gradual movement toward the central axis during the loading.

AUTHOR INFORMATION

Corresponding Author

Serhiy Pyshyev − *Lviv Polytechnic National University, Lviv 79013, Ukraine;* orcid.org/0000-0003-0737-1122; Email: gajva@polynet.lviv.ua

Authors

Yevgen Zbykovskyy − *Donetsk National Technical University, Pokrovsk 85300, Ukraine;* orcid.org/0000-0001-7429-3844

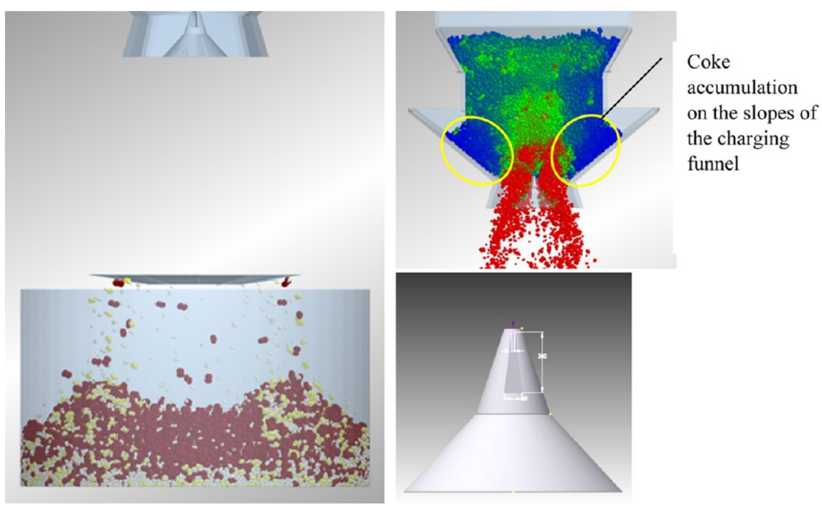

Figure 25. Formation of the saddle-shaped gap.

https://doi.org/10.1021/acsomega.3c00747
ACS Omega 2023, 8, 19464−19473

Iryna Shvets − *Donetsk National Technical University, Pokrovsk 85300, Ukraine;* orcid.org/0000-0001-7386-3286

Denis Miroshnichenko − *Kharkiv Polytechnic Institute, National Technical University, Kharkiv 61002, Ukraine;* orcid.org/0000-0002-6335-8742

Sergiy Kravchenko − *State Enterprise "State Institute for Designing Enterprises of Coke Oven and By-Product Plants (GIPROKOKS)", Kharkiv 61002, Ukraine*

Stanislav Stelmachenko − *State Enterprise "State Institute for Designing Enterprises of Coke Oven and By-Product Plants (GIPROKOKS)", Kharkiv 61002, Ukraine;* orcid.org/0009-0002-6034-9258

Yuriy Demchuk − *Lviv Polytechnic National University, Lviv 79013, Ukraine;* orcid.org/0000-0001-7983-5067

Nataliya Vytrykush − *Lviv Polytechnic National University, Lviv 79013, Ukraine;* orcid.org/0000-0001-8437-0153

Complete contact information is available at: https://pubs.acs.org/10.1021/acsomega.3c00747

Notes

The authors declare no competing financial interest.

■ ACKNOWLEDGMENTS

This publication of research results was supported by the German Academic Exchange Service (DAAD) under the Program "Ukraine digital: Ensuring academic success in times of crisis (2022)" in partnership with the University of Stuttgart.

■ REFERENCES

(1) Miroshnichenko, D. V.; Desna, N. A.; Kaftan, Y. S. Oxidation of coal in industrial conditions. 2. Modification of the plastic and viscous properties on oxidation. *Coke Chem.* **2014**, *57*, 375−380.

(2) Shmeltser, E. O.; Lyalyuk, V. P.; Sokolova, V. P.; Miroshnichenko, D. V. The using of coal blends with an increased content of coals of the middle stage of metamorphism for the production of the blastfurnace coke. Message 1. Preparation of coal blends. *Petroleum and Coal* **2018**, *60* (4), 605−611.

(3) Sajwan, K. S.; Punshon, T.; Seaman, J. C. Production of Coal Combustion Products and Their Potential Uses. In *Coal Combustion Byproducts and Environmental Issues*; Sajwan, K. S., Twardowska, I., Punshon, T., Alva, A. K., Eds.; Springer: New York, NY, 2006, 3−9.

(4) Siddique, R. Utilization of coal combustion by-products in sustainable construction materials. *Resour. Conserv. Recycl.* **2010**, *54*, 1060−1066.

(5) Li, J.; Zhuang, X.; Querol, X.; Font, O.; Moreno, N. A review on the applications of coal combustion products in China. *Int. Geol. Rev.* **2018**, *60*, 671−716.

(6) Pyshyev, S.; Prysiazhnyi, Y.; Borbeyiyong, G. I.; Chervinskyy, T.; Kułażyński, M.; Grytsenko, Y. Effect of raw material composition on the properties of road asphalt modifier obtained from liquid coal coking products. *Przem. Chem.* **2021**, *100*, 680.

(7) Pyshyev, S.; Demchuk, Y.; Poliuzhyn, I.; Kochubei, V. Obtaining and use adhesive promoters to bitumen from the phenolic fraction of coal tar. *Int. J. Adhes. Adhes.* **2022**, *118*, 103191.

(8) Feng, Y.; Zhang, X.; Yu, Q.; Shi, Z.; Liu, Z.; Zhang, H.; Liu, H. Experimental and numerical investigations of coke descending behavior in a coke dry quenching cooling shaft. *Appl. Therm. Eng.* **2008**, *28*, 1485−1490.

(9) Li, Z.; Zhang, X.; Lai, N. C.; Jiang, Z.; Li, J. A novel process for coke wastewater gasification quenching: Energy and exergy analysis. *Appl. Therm. Eng.* **2021**, *191*, 116863.

(10) Shulga, I. V.; Miroshnichenko, D. V.; Pyshyev, S. V.; Bogoyavlenska, O. V. *Coke Production. Kharkiv- Ternopil: NTU "KhPI"*; Krok Publishing House, 2022; 110.

(11) Miroshnichenko, D. V.; Ulanovskiy, M. L. *Reactivity of coke: Methods of measuring and influence factors*; Koks I Khimiya, 2004; 21.

(12) Li, Z.; Zhang, X.; Jiang, Z.; Wu, L.; Lai, N. C. Bi-objective optimization and thermal economy analysis of a novel coke quenching process with wastewater gasification. *Appl. Therm. Eng.* **2023**, *219*, 119473.

(13) Errera, M. R.; Milanez, L. F. Thermodynamic analysis of a coke dry quenching unit. *Energy Convers. Manag.* **2000**, *41*, 109−127.

(14) Zhang, M.; Han, C.; Ni, K.; Gu, H.; Huang, A.; Yu, C. In situ synthesis of AlN whiskers in mullite-silicon carbide refractory under simulated coke dry quenching conditions. *Ceram. Int.* **2018**, *44*, 5945−5949.

(15) Sun, K.; Tseng, C. T.; Shan-Hill Wong, D.; Shieh, S. S.; Jang, S. S.; Kang, J. L.; Hsieh, W. D. Model predictive control for improving waste heat recovery in coke dry quenching processes. *Energy* **2015**, *80*, 275−283.

(16) Wang, J. G.; Xie, Z.; Yao, Y.; Yang, B. H.; Ma, S. W.; Liu, L. L. Soft sensor development for improving economic efficiency of the coke dry quenching process. *J. Process Control* **2019**, *77*, 20−28.

(17) Wang, J. G.; Wang, Y.; Yao, Y.; Yang, B. H.; Ma, S. W. Stacked autoencoder for operation prediction of coke dry quenching process. *Control Eng. Pract.* **2019**, *88*, 110−118.

(18) Bannikov, L.; Miroshnichenko, D.; Pylypenko, O.; Pyshyev, S.; Fedevych, O.; Meshchanin, V. Coke quenching plenum equipment corrosion and its dependents on the quality of the biochemically treated water of the coke-chemical production. *Chem. Chem. Technol.* **2022**, *16*, 328−336.

(19) Grebenyuk, A. F.; Zbykovskii, A. I. *Calculations of coke production processes/Design guide*; Donetsk: Nord-Press, 2008, 322.